Burns & Trauma, 2024, 12, tkae010
https://doi.org/10.1093/burnst/tkae010
Research Article

OXFORD

Research Article

Acidic fibroblast growth factor inhibits reactive oxygen species-induced epithelial–mesenchymal transdifferentiation in vascular endothelial cells via the miR-155-5p/SIRT1/Nrf2/HO-1 pathway to promote wound healing in diabetic mice

Yue Zhang[†], Fenghui Hei[†], Yujie Xiao, Yang Liu, Juntao Han, Dahai Hu[*] and Hongtao Wang[*]

Department of Burns and Cutaneous Surgery, Xijing Hospital, Fourth Military Medical University, 127 Changle West Road, Xi'an, Shaanxi 710032, China

[*]Correspondence. Dahai Hu, Email: hudhai@fmmu.edu.cn; Hongtao Wang, Email: wanght@fmmu.edu.cn

[†]Yue Zhang and Fenghui Hei contributed equally to this work.

Received 22 October 2023; Revised 19 February 2024; Accepted 22 February 2024

Abstract

Background: Diabetic chronic wounds are among the most common and serious complications of diabetes and are associated with significant morbidity and mortality. Endothelial-to-mesenchymal transition (EndMT) is a specific pathological state in which endothelial cells are transformed into mesenchymal cells in response to various stimuli, such as high glucose levels and high oxidative stress. Acidic fibroblast growth factor (aFGF), which is a member of the fibroblast growth factor family, possesses strong antioxidant properties and can promote the differentiation of mesenchymal stem cells into angiogenic cells. Therefore, we investigated the role of aFGF in EndMT in diabetic wounds and analysed the underlying mechanisms.

Methods: A diabetic mouse model was used to verify the effect of aFGF on wound healing, and the effect of aFGF on vascular endothelial cells in a high-glucose environment was examined *in vitro*. We examined the expression of miR-155-5p in a high-glucose environment and the miR-155 downstream target gene SIRT1 by luciferase reporter assays.

Results: aFGF promoted wound closure and neovascularization in a mouse model of type 2 diabetes. *In vitro*, aFGF inhibited the production of total and mitochondrial reactive oxygen species (ROS) in vascular endothelial cells and alleviated epithelial–mesenchymal transdifferentiation in a high-glucose environment. Mechanistically, aFGF promoted the expression of SIRT1 and the downstream targets Nrf2 and HO-1 by negatively regulating miR-155-5p, thereby reducing ROS generation.

Conclusions: In conclusion, our results suggest that aFGF inhibits ROS-induced epithelial–mesenchymal transdifferentiation in diabetic vascular endothelial cells via the miR-155-5p/SIRT1/Nrf2/HO-1 axis, thereby promoting wound healing.

Key words: EndMT, Acidic fibroblast growth factor, Reactive oxygen species, Chronic wounds, Wound healing, Diabetic wound, Fibroblast

© The Author(s) 2024. Published by Oxford University Press.
This is an Open Access article distributed under the terms of the Creative Commons Attribution Non-Commercial License (https://creativecommons.org/licenses/by-nc/4.0/), which permits non-commercial re-use, distribution, and reproduction in any medium, provided the original work is properly cited. For commercial re-use, please contact journals.permissions@oup.com

Downloaded from academic.oup.com/burnstrauma/article/doi/10.1093/burnst/tkae010/7683168 by guest on 13 October 2026

Highlights

- This study showed that aFGF inhibited epithelial–mesenchymal transdifferentiation in HUVECs induced by high glucose concentrations.
- This study confirmed that aFGF inhibited EndMT in diabetic vascular endothelial cells via the miR-155-5p/SIRT1/Nrf2/HO-1 axis.
- This study will be helpful for further understanding the relationship between aFGF and VE cell dysfunction in diabetic wounds, thereby providing support for treating chronic diabetic wounds.

Background

According to the latest data released by the International Diabetes Federation, there are currently >537 million people with diabetes worldwide. The incidence of diabetic wounds is ~8.1%, and a higher incidence has been reported in the lower extremities due to poor blood circulation [1]. Wound healing in diabetic patients is difficult, and the amputation (toe) rate is as high as 14–24%; this is one of the most serious complications of diabetes [2]. The main characteristics of these types of wounds are excessive oxidative stress and decreased antioxidant capacity caused by sustained hyperglycaemia. This leads to an excessive increase in reactive oxygen species (ROS), thereby inhibiting neovascularization and collagen deposition; thus, wound healing is either delayed or prevented [3,4]. High oxidative stress in diabetic wounds can induce endothelial-to-mesenchymal transition (EndMT), resulting in significant changes in the polarity, morphology and function of endothelial cells (ECs) [5]. This conversion is characterized by a reduction in the tight junctions of ECs, the extravasation of substances in blood vessels and an increase in local inflammatory reactions [6]. In addition to the accumulation of extracellular matrix components such as collagen and smooth muscle actin (SMA), vascular fibrosis can occur, and narrowing or even blockade of the lumen. These alterations aggravate wound ischaemia and inhibit wound healing. The expression of specific markers, such as vascular endothelial (VE) cadherin and Platelet endothelial cell adhesion molecule-1 (CD31), is reduced, whereas the expression of mesenchymal markers, such as α-SMA and vimentin (Vim), is increased [7]. EndMT is a reversible process that is involved in many pathological and physiological processes, including embryonic development, angiogenesis and the local infiltration and distant migration of tumour cells. Under certain conditions, mesenchymal cells that undergo EndMT can be transformed back to ECs. However, in a sustained high-glucose environment, mesenchymal cells that undergo EndMT cannot be transformed back into ECs and cannot form functional new blood vessels [8,9]. EndMT is an important factor that hinders neovascularization.

Acidic fibroblast growth factor (aFGF), which is also known as FGF1, was the first member of the fibroblast growth factor (FGF) family identified. It promotes embryonic development, wound healing and vascular regeneration, and regulates immune metabolism [10]. Currently, aFGF is considered an angiogenic factor [11]. Clinical studies have also indicated that aFGF can promote wound healing by increasing the density of new blood vessels and ameliorating wound ischaemia and hypoxia [12]. Following vascular injury caused by oxidative stress and other factors, aFGF expression is significantly increased in human umbilical vein endothelial cells (HUVECs) and vascular smooth muscle cells, thereby activating nitric oxide synthase, increasing capillary permeability and alleviating vasodilation and vasospasm [13]. These findings suggest that an increase in aFGF expression is an adaptive response and may exert a protective effect, and controlling the expression of aFGF in the vascular wall can be used to regulate the formation of new blood vessels. Recent studies have indicated that under high oxidative stress conditions, aFGF can promote the migration of mesenchymal stem cells to wounds. Furthermore, aFGF can enhance the differentiation of bone marrow mesenchymal stem cells and adipose mesenchymal stem cells into HUVECs [14,15]. aFGF further participates in the formation of new blood vessels, thereby suggesting a new approach to reverse EndMT in diabetic wounds and improve angiogenesis.

Various microRNAs (miRNAs) (miR-21, miR-132, miR-146a, miR-200, miR-210 and miR-155) are differentially expressed under conditions associated with diabetic wounds. These miRNAs play key roles in diabetic wound healing by regulating inflammation, proliferation and remodelling pathways [16]. Abnormally expressed miRNAs may affect the diabetic wound healing process [17]. The expression of miR-155, which is a noncoding small RNA that is involved in wound oxidative stress, is significantly increased in high-glucose environments. Inhibiting miR-155 can significantly improve wound healing in diabetes [18]. Therefore, we focused on the specific mechanisms by which aFGF and miR-155 affect diabetic vascular complications and their relationship with EndMT. Our results indicated that aFGF could reduce local ROS accumulation and ameliorate EndMT by negatively regulating miR-155-5p. Furthermore, bioinformatics analysis and the prediction results confirmed the presence of a complementary binding site between sirtuin 1 (SIRT1) and miR-155-5p. Finally, we verified that the Nuclear Factor erythroid 2-Related Factor 2/Heme Oxygenase-1 (Nrf2/HO-1) pathway, which is a classic pathway that regulates oxidative stress, can be promoted by SIRT1 through the inhibition of miR-155-5p. Thus, the Nrf2/HO-1 pathway was positively regulated, ROS clearance was promoted, oxidative stress was alleviated, and ultimately, ROS-induced EndMT in diabetic HUVECs was inhibited, thereby promoting wound healing. In conclusion, our work provides a new and rational

Downloaded from academic.oup.com/burnstrauma/article/doi/10.1093/burnst/tkae010/7683168 by guest on 13 October 2026

explanation for the therapeutic efficacy of aFGF in treating diabetic wounds.

Methods

Animal models

Db/db mice (~6 weeks old) were obtained from Cavens (ChangZhou, China). Blood glucose levels in samples collected from the tail vein were measured with a One-Touch blood glucose meter (Johnson, USA) and the blood glucose levels were >16.7 mmol/l. A round full-thickness skin wound was created by surgical scissors after the animals were anesthetized. The diameter of the wound was 10 mm. Beginning 1 day later, 0.5 ml of phosphate-buffered saline (PBS) or aFGF (200 μg) diluted with 0.5 ml of PBS was administered into the wound by subcutaneous injection for a five consecutive days. The size of the wound was subsequently measured and recorded by digital photographs at the indicated times. After the mice were sacrificed, the wound tissues were harvested for subsequent experiments. There were five mice in each experimental group (n = 5).

Immunohistochemistry and immunofluorescence staining of skin tissue

Mouse skin tissue was harvested and fixed in 4% formaldehyde or frozen for sectioning (−80°C). The skin was sectioned into 4-μm-thick slices. Then, the tissues were subjected to Masson's trichrome, haematoxylin/eosin (H&E) and immunofluorescence staining. The fixed sections were stained with CD31 and α-SMA antibodies (1 : 200; Abcam, Cambridge, UK). ROS dye solution (Beyotime, Shanghai, China) was used to determine ROS levels in skin tissues and 4',6-diamidino-2-phenylindole (DAPI) (Beyotime, Shanghai, China) was used to stain the nuclei. Images were obtained using an FSX100 microscope (Olympus, Tokyo, Japan).

Cell culture, treatment and transfection

HUVECs were obtained from the China Center for Type Culture Collection. The cells were cultured in dulbeccos modified eagle medium (DMEM) (Gibco, Grand Island, NY, USA) supplemented with 10% fetal bovine serum (Corning, USA), 100 U/ml penicillin and 100 μg/ml streptomycin. The cells were incubated at 37°C with 5% CO_2. After they had reached 80% confluence, the cells were used for subsequent experiments. HUVECs were exposed to high glucose (33 mM) for 24 h to mimic diabetes.

To mimic or silence miR-155-5p, HUVECs were transfected with the miR-155-5p mimic or small interfering RNA (siRNA) purchased from Santa Cruz Biotechnology (Santa Cruz, CA, USA). Lipofectamine 2000 reagent (Invitrogen, Life Technologies, Grand Island, NE, USA) was used for 12 h according to the manufacturer's instructions, and negative control siRNA was used as a control. The transfection efficiency was measured by RT–PCR at 24 h.

Proliferation, migration and tube formation assays

To evaluate the effect of aFGF on HUVECs under high-glucose conditions, cell proliferation, migration and tube formation assays were performed. Ki67 immunofluorescence staining was used to evaluate cell proliferation. After fixation with 4% paraformaldehyde and permeabilization with 0.1% Triton X-100, the cells were stained with anti-Ki67 antibodies (1 : 200; Abcam, Cambridge, UK) and probed with an AF488-conjugated secondary antibody (1 : 100; Abcam, Cambridge, UK). The number of Ki67-positive cells was subsequently counted by ImageJ software.

HUVECs were seeded in a 6-well plate at a density of $\sim 1 \times 10^6$/well. A scratch was induced with a 10 μl pipette tip. The cells were photographed at 0, 12 and 24 h by an FSX100 microscope (Olympus, Tokyo, Japan).

The effects of aFGF in each group were evaluated by cell migration and tube formation assays. Briefly, cells (4×10^4) were added to the upper chamber of a transwell assay filter. After being cultured for 8 h at 37°C, the cells were fixed, stained with 0.5% crystal violet, photographed and examined with ImageJ software.

Mitochondrial membrane potential analysis

JC-1 staining solution was used according to the manufacturer's instructions (Beyotime, Shanghai, China); the cells were incubated for 30 min and then washed twice with JC-1 buffer. The mitochondrial membrane potential (MMP) was calculated by determining the ratio of red to green fluorescence.

Intracellular ROS and mitochondrial ROS measurements

HUVEC ROS levels were examined with an ROS assay kit (Beyotime, Shanghai, China) according to the manufacturer's instructions. Briefly, 2 μmol/l dihydroethidium was added to the cells and incubated at 37°C for 30 min, after which the relative levels of cellular ROS were measured by an FSX100 microscope. Intracellular and mitochondrial ROS (mtROS) concentrations were monitored by MitoSOX™ Red mitochondrial superoxide indicator (Thermo Fisher, Waltham, MA, USA).

Immunofluorescence staining of HUVECs

The cells were fixed with 4% paraformaldehyde, permeabilized with 0.3% Triton X-100, blocked with 10% goat serum albumin, and stained with Ki67, CD31, α-SMA, VE-cadherin and Vim antibodies (1 : 200; Abcam, Cambridge, UK) at 4°C overnight. Then, goat anti-rabbit and goat anti-mouse secondary antibodies (1 : 100; Abcam) were added and incubated at 37°C for 1 h. Finally, DAPI staining was performed and the cells were observed by an FSX100 microscope.

Western blot analysis of HUVECs

The proteins were isolated from HUVECs, separated by sodium dodecyl sulfate-polyacrylamide gel electrophoresis

Downloaded from academic.oup.com/burnstrauma/article/doi/10.1093/burnst/tkae010/7683168 by guest on 13 October 2026

Table 1.

5'	...AGGAAUUGUUCCACCAGCAUUAG...
	|||||||
3'	UGGGGAUAGUGCUAAUCGUAAUU

(SDS-PAGE) and transferred to polyvinylidene fluoride membranes (Millipore, Billerica, MA, USA). Then, the membranes were blocked with 5% nonfat dry milk for ~2 h and incubated with antibodies against CD31, α-SMA, VE-cadherin and Vim (1 : 200; Abcam, Cambridge, UK) at 4°C overnight. β-Actin (1 : 3000; Abcam, Cambridge, UK) was used as a control. The membranes were washed three times and incubated with Horseradish PeroxidaseHRP-conjugated anti-rabbit IgG secondary antibodies (1 : 2000; Boster, Wuhan, China) for 1 h at 37°C. An Electrochemiluminescence (ELC) detection system (Millipore, USA) was used and the band intensity was examined with a FluorChem FC system (Alpha Innotech). The results were normalized against β-actin, and ImageJ software was used to analyse the results.

The proteins that can be separated by 10% SDS-PAGE are 50–110 kDa in length. When the proteins were larger than 100 kDa, 8% SDS–PAGE was performed. In our study, the expression of VE-cadherin (130–140 kDa), CD31 (130 kDa), α-SMA (42 kDa), Vim (57 kDa), Sirt1 (120 kDa), Nrf2 (97–100 kDa) and HO-1 (33 kDa) was evaluated. Therefore, VE-cadherin, CD31 and Sirt1 were examined by 8% SDS-PAGE and the remaining proteins were examined by 10% SDS-PAGE.

Luciferase reporter assay

To confirm that SIRT1 was a direct target of miR-155-5p, we generated luciferase-3′-untranslated region (3′UTR) reporter constructs of SIRT1 mRNA. The wild-type SIRT1 3′UTR, the mutant SIRT1 3′UTR or the corresponding nontargeting control RNA was cotransfected with miR-155-5p mimics. The specific loci at which miR155-5p matched SIRT1 is shown in Table 1. The samples were obtained 24 h after transfection and used for luciferase assays (Promega, WI, USA).

Statistical analysis

The data were analysed using SPSS 26.0 software and the means ± SD are presented. Student's t test was used for comparisons between two groups. Multiple groups were analysed by two-way analysis of variance with Tukey's *post hoc* test. In all the cases, if $p < 0.05$, there was a significant difference.

Results

aFGF promotes wound healing in diabetic mice

First, we established a wound model in diabetic db/db mice with fasting blood glucose levels >16.7 mmol/l, as measured in tail vein blood. A 10 mm diameter full-layer skin injury was established on the backs of the mice, and 100 μl of PBS (control) or 200 μg of aFGF was injected subcutaneously around the wound for five consecutive days. At each time point, the skin wound area in the aFGF treatment group was smaller than that in the control group, and the wounds in the aFGF group were mostly closed by day 14 (Figure 1A–C). We performed Masson and H&E staining of the wound samples to histologically evaluate the contraction of the wound base, granulation and epithelial processes on day 14. Masson staining revealed the collagen profile in the wounds in the two groups (Figure 1D). Compared with those in the control group, the collagen fibres in the aFGF group were arranged in a regular and orderly manner. H&E staining revealed that the granulation tissue in the aFGF group had healed well, the wound length was the shortest and epithelial tissue had fully formed (Figure 1E). H&E and Masson staining showed that aFGF could effectively treat diabetic wounds. Furthermore, ROS fluorescence staining was performed on the skin tissue from the wounds on day 14 (Figure 1F). The ROS fluorescence intensity in the aFGF group was significantly lower than that in the control group, suggesting that aFGF effectively reduced the level of ROS in wounds and ameliorated oxidative stress in diabetic wounds. On day 14 after wound formation, the α-SMA/CD31 dual-fluorescence results revealed that there were more blood vessels in the aFGF group than in the control group, as indicated by the increases in vascular density and the number of blood vessels, the large lumens and structural integrity (Figure 1G–I). These findings confirmed that aFGF could promote angiogenesis and vessel maturation. Thus, aFGF reduced ROS levels in wounds, promoted angiogenesis and accelerated the healing of diabetic wounds.

aFGF inhibits epithelial–mesenchymal transdifferentiation of HUVECs induced by high glucose concentrations

We examined the effect of aFGF on HUVECs in a high-glucose environment *in vitro*. HUVECs in a high-glucose environment were immunofluorescently stained for Ki67, which is a common biomarker used to evaluate cell proliferation, and the aFGF group exhibited the strongest Ki67-positive staining (Figure 2A, C). Similarly, the aFGF group exhibited more cell migration than the other group (Figure 2B, D, G, L). Additionally, the highest amount of tube formation and complete tubular structures were observed in HUVECs in this group (Figure 2H, K). Therefore, aFGF promoted the proliferation and migration of HUVECs and tube formation in high-glucose environments. In these environments, ROS are produced by factors such as nicotinamide adenine dinucleotide phosphate oxidase, xanthine oxidase and other pathways, and mitochondria are the main source of ROS production in cells. When glucose levels are high, mitochondria can increase ROS production, which leads to cellular oxidative stress and tissue damage. Therefore, we

Downloaded from academic.oup.com/burnstrauma/article/doi/10.1093/burnst/tkae010/7683168 by guest on 13 October 2026

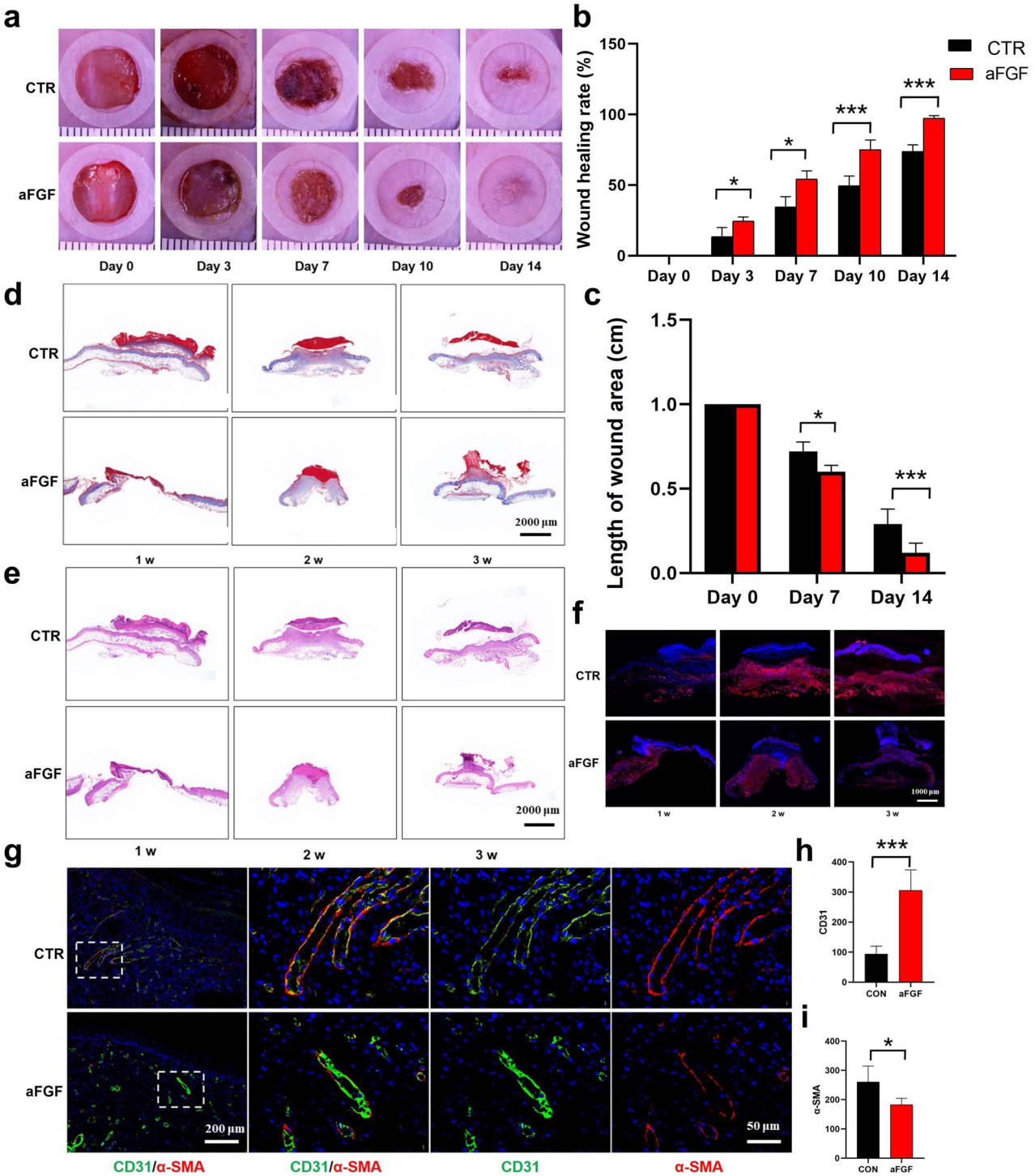

Figure 1. Effects of aFGF on wound healing in a diabetic mouse model. (**a**) Digital images of wounds treated with PBS or aFGF on days 0, 3, 7, 10 and 14. (**b**) Analysis of the wound closure rate in each group at each time point. (**c**) Analysis of the wound length on days 0, 7 and 14 in each group. (**d**) Representative Masson staining of the wound tissue in each group on 1 week, 2 week and 3 week; scale bar: 2000 μm. (**e**) Representative H&E staining results of the wound tissue in each group on day 14; scale bar: 2000 μm. (**f**) Representative images of ROS levels in skin wound tissue; scale bar: 1000 μm. (**g**) Representative images of α-SMA and CD31 immunofluorescence staining of skin wound tissue on day 14 after injury; scale bar: 200 μm (left) and scale bar: 50 μm (enlarged). Statistical analysis of the relative expression of (**h**) CD31 and (**i**) α-SMA (n = 5 per group, $^{*}p < 0.05$, $^{***}p < 0.001$). *CTR* control, *aFGF* acidic fibroblast growth factor, *ROS* reactive oxygen species, *α-SMA* α-smooth muscle actin

Downloaded from academic.oup.com/burnstrauma/article/doi/10.1093/burnst/tkae010/7683168 by guest on 13 October 2026

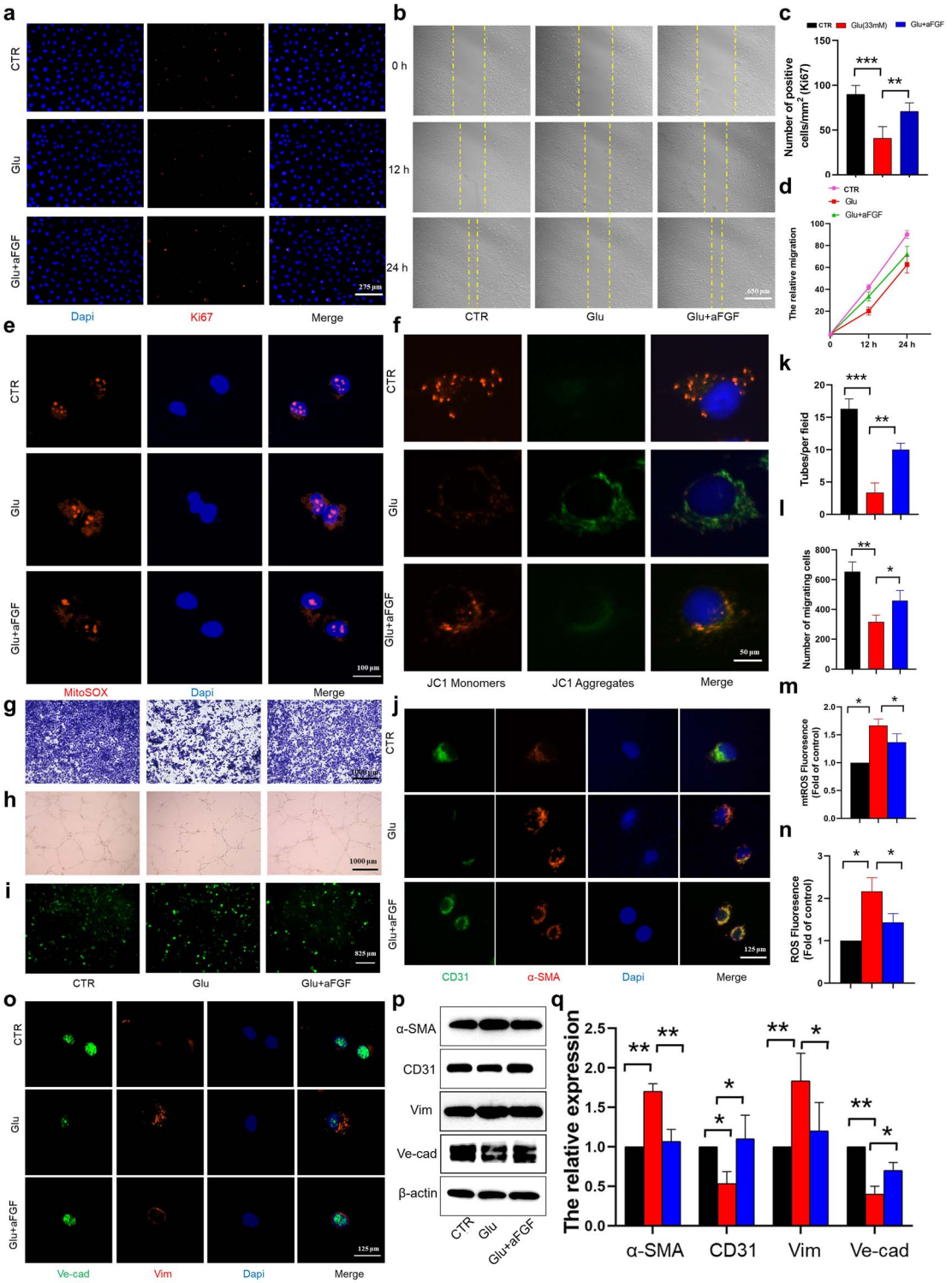

Figure 2. Effects of aFGF on EndMT in HUVECs. (**a**) The effect of aFGF on HUVEC proliferation was determined using Ki67 immunofluorescence assays; scale bar: 275 μm. (**b**) Effect of aFGF on HUVEC migration at each time point; scale bar: 650 μm. (**c**) Statistical analysis of the relative Ki67 expression in the different groups. (**d**) Relative migration of HUVECs in each group. (**e**) Mitochondrial ROS levels in HUVECs in the different groups; scale bar: 100 μm. (**f**) The JC-1 signal in HUVECs was examined by fluorescence confocal microscopy. The cells were labelled with JC-1 to show mitochondria. Double staining of cells stained with JC-1 is shown: green for J-monomers and red for J-aggregates (scale bar: 50 μm). (**g**) The effect of aFGF on HUVEC migration was examined using a transwell assay after 8 h of coculture; scale bar = 1000 μm. (**h**) Angiogenesis in the different groups; scale bar: 1000 μm. (**i**) HUVEC ROS levels in the different groups were examined using immunofluorescence assays; scale bar: 825 μm. (**j**, **o**) Immunofluorescence analysis of CD31, α-SMA, VE-cadherin and vimentin in the different groups; scale bar: 125 μm. (**k**) Quantification of the number of tubes per field. (**l**) Quantification of the number of migrated HUVECs. (**m**) Quantitative analysis of mtROS levels in HUVECs in each group. (**n**) Quantitative analysis of HUVEC ROS levels in each group. (**p**, **q**) Western blot analysis of α-SMA, CD31, vimentin and VE-cadherin expression (n = 3 per group, $^{*}p < 0.05$, $^{**}p < 0.01$, $^{***}p < 0.001$). *N* normal, *Glu* glucose, *Vim* vimentin, *Ve-cad* VE-cadherin, *aFGF* acidic fibroblast growth factor, *ROS* reactive oxygen species, α-*SMA* α-smooth muscle actin

Downloaded from academic.oup.com/burnstrauma/article/doi/10.1093/burnst/tkae010/7683168 by guest on 13 October 2026

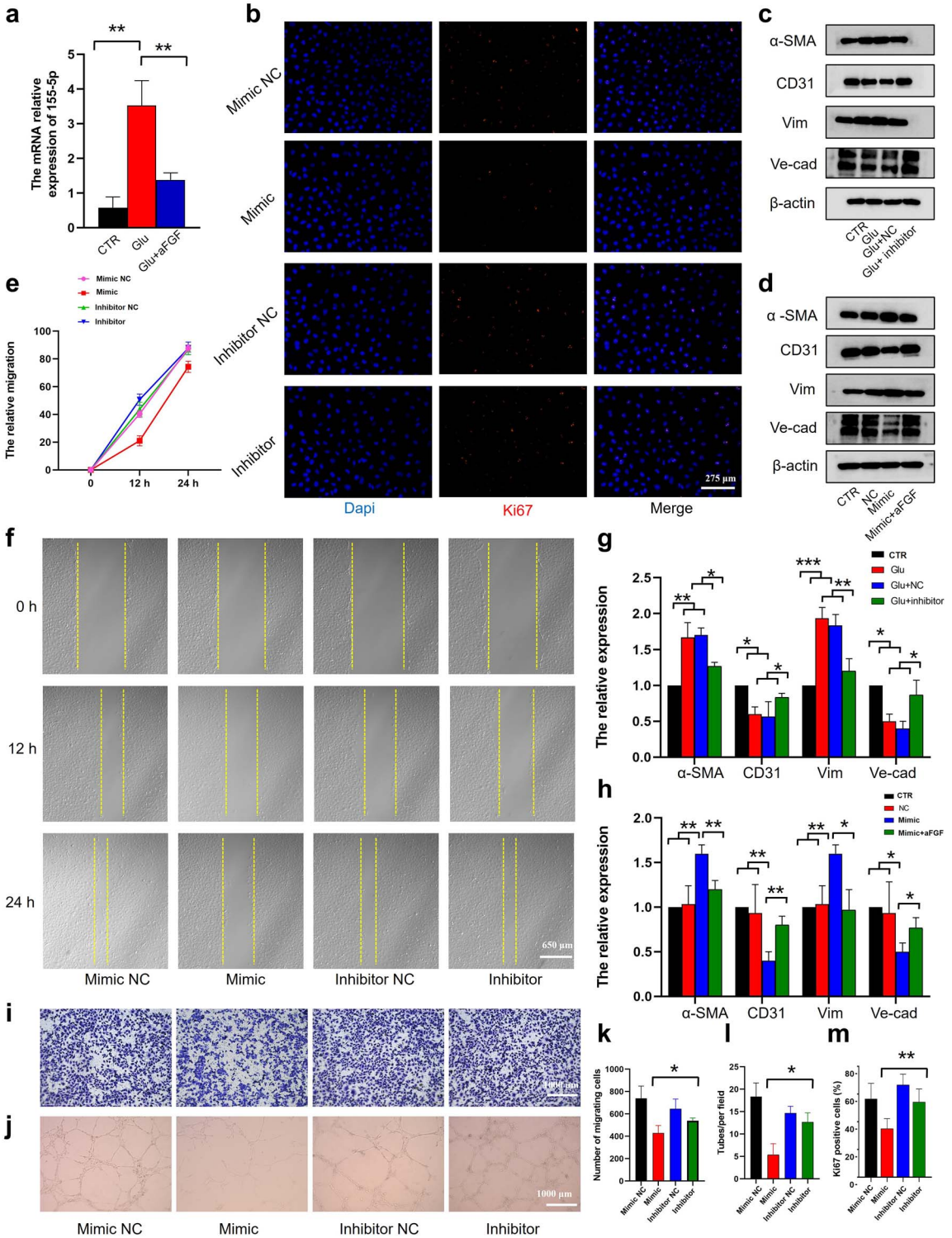

Figure 3. aFGF inhibits EndMT through miR155-5p in HUVECs. (**a**) Levels of miR155-5p in HUVECs in high-glucose environments were analysed by qRT–PCR. (**b**) Effect of miR155-5p on HUVEC proliferation was determined using Ki67 immunofluorescence assays; scale bar: 275 μm. (**c**, **d**) Western blot results showing the expression of α-SMA, CD31, vimentin and VE-cadherin in the different groups. (**e**) Relative migration of HUVECs in each group. (**f**) Effect of miR155-5p on HUVEC migration at each time point; scale bar: 650 μm. (**g**, **h**) Statistical analysis of the protein expression of α-SMA, CD31, vimentin and VE-cadherin. (**i**) The effect of miR155-5p on HUVEC migration was examined using a Transwell assay after 8 h of coculture; scale bar: 1000 μm. (**j**) Angiogenesis in the different groups; scale bar: 1000 μm. (**k**) Quantification of the number of migrated HUVECs. (**l**) Quantification of the number of tubes per field. (**m**) Statistical analysis of the relative Ki67 expression in the different groups. (n = 3 per group, $^{*}p < 0.05$, $^{**}p < 0.01$, $^{***}p < 0.001$). *N* Normal, *Glu* glucose, *NC* negative control, *Mimic NC* mimic negative control, *Inhibitor NC* inhibitor negative control, *Vim* vimentin, *Ve-cad* VE-cadherin,*aFGF* acidic fibroblast growth factor, α-*SMA* α-smooth muscle actin

Downloaded from academic.oup.com/burnstrauma/article/doi/10.1093/burnst/tkae010/7683168 by guest on 13 October 2026

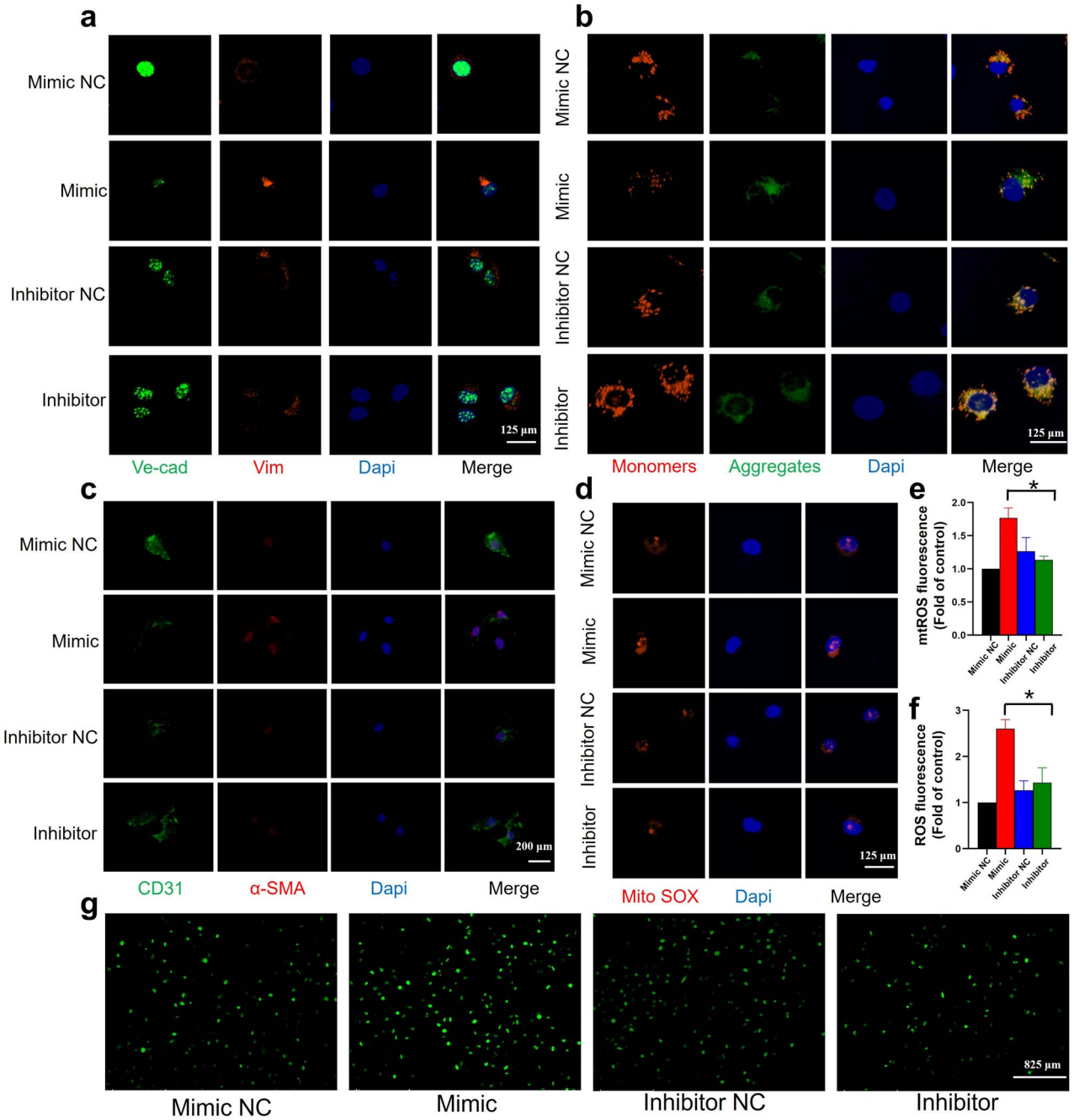

Figure 4. aFGF reduces ROS production in a high-glucose environment, partially ameliorating EndMT in HUVECs. (**a**) Immunofluorescence staining of vimentin and VE-cadherin in the different groups; scale bar = 125 μm. (**b**) JC-1 signals in HUVECs in the different groups were examined by fluorescence confocal microscopy; scale bar = 125 μm. (**c**) Immunofluorescence staining of CD31 and α-SMA in the different groups; scale bar = 200 μm. (**d**) mtROS levels in HUVECs in the different groups were examined using immunofluorescence assays; scale bar =125 μm. (**e**) Quantitative analysis of mtROS levels in HUVECs in each group. (**f**) Quantitative analysis of ROS levels in HUVECs in each group. (**g**) ROS levels in HUVECs in the different groups were examined using immunofluorescence assays; scale bar = 825 μm. (n = 3 per group, $^{*}p < 0.05$). *NC* negative control, *Ve-cad* VE-cadherin, *Vim* vimentin, *Mito SOX* mitochondrial superoxide indicator, *aFGF* acidic fibroblast growth factor, *ROS* reactive oxygen species

performed fluorescence staining to evaluate the total ROS and mtROS levels in cells, and the results showed that ROS and mtROS levels were significantly increased in cells exposed to high glucose. aFGF pretreatment inhibited the production of ROS and mtROS in these cells (Figure 2I, E, M, N). JC-1 staining was used to evaluate the protective effect of aFGF on mitochondria in HUVECs under high-glucose conditions. Compared with that in the control group, the MMP in the high-glucose group was significantly reduced, and pretreatment with aFGF prevented the loss of the MMP and reduced mitochondrial damage (Figure 2F). Under high oxidative-stress conditions, HUVECs underwent EndMT, which

Downloaded from academic.oup.com/burnstrauma/article/doi/10.1093/burnst/tkae010/7683168 by guest on 13 October 2026

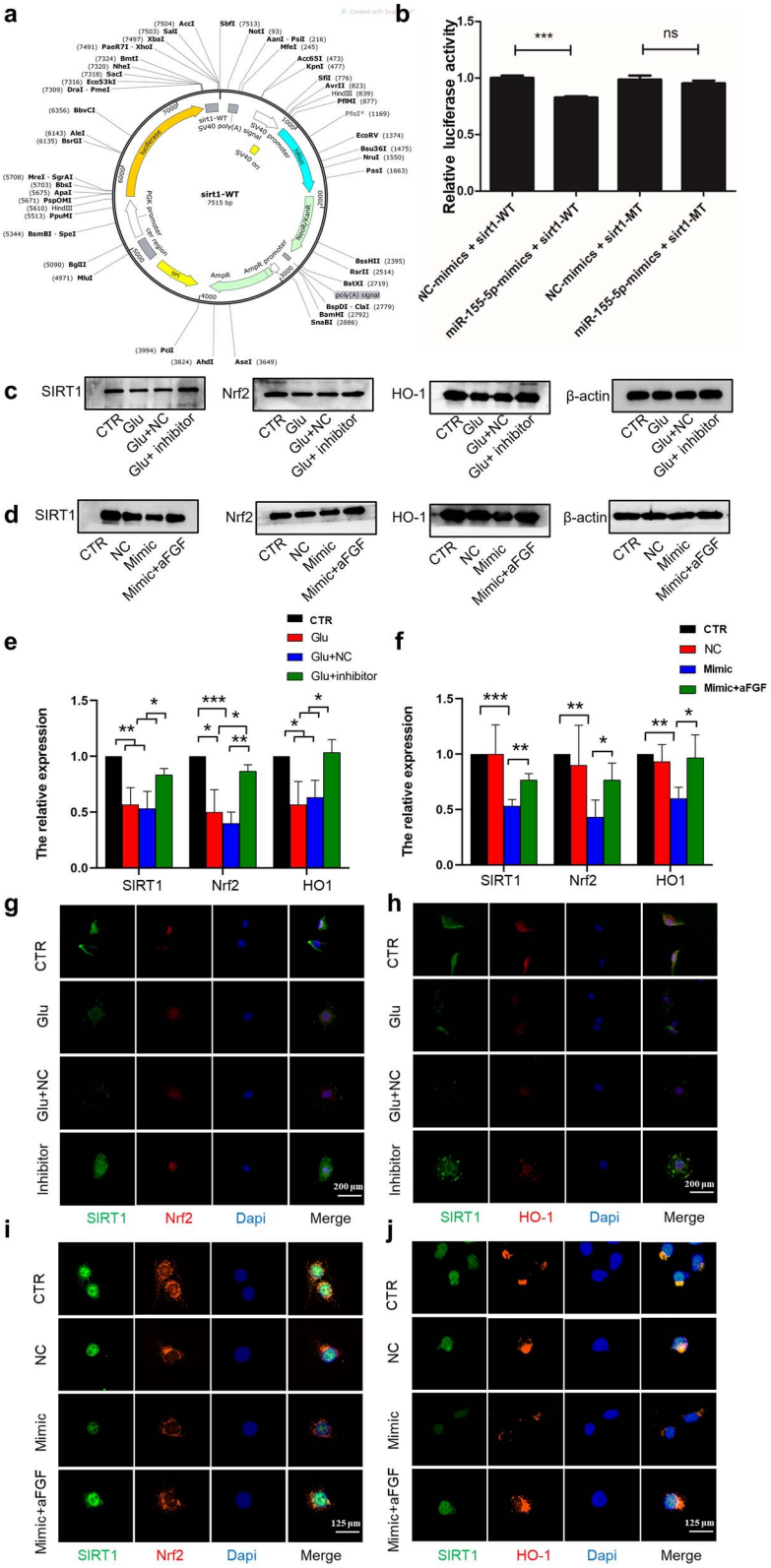

Figure 5. Verification of the targeted regulatory relationship between miR155-5p and SIRT1 in HUVECs. (**a**, **b**) Targeted modulation was measured by luciferase reporter gene assays. (**c**, **d**) Western blot results showing SIRT1, Nrf2 and HO-1 expression in the different groups. (**e**, **f**) Statistical analysis of SIRT1, Nrf2 and HO-1 expression. (**g**, **h**) Immunofluorescence staining of SIRT1, Nrf2 and HO-1 in the inhibitor groups; scale bar: 200 μm. (**i**, **j**) Immunofluorescence staining of SIRT1, Nrf2 and HO-1 in the mimic groups; scale bar: 125 μm. (n = 3 per group, $^{*}p < 0.05$, $^{**}p < 0.01$, $^{***}p < 0.001$). *WT* Wild type, *MT* mutation type, *Nrf2* recombinant nuclear respiratory factor 1, *HO-1* heme oxygenase 1, *N* normal, *Glu* glucose, *NC* negative control

Downloaded from academic.oup.com/burnstrauma/article/doi/10.1093/burnst/tkae010/7683168 by guest on 13 October 2026

hindered their function and affected neovascularization and wound healing. Fluorescence and protein expression assays confirmed that in high-glucose environments, the expression of the vascular EC-specific markers VE-cadherin and CD31 was decreased, whereas the expression of the mesenchymal markers α-SMA and Vim was increased. aFGF partially reversed these pathological changes (Figure 2J, O, P, Q). These findings partly confirmed that aFGF promoted neovascularization in high-glucose environments and inhibited the epithelial–mesenchymal transdifferentiation of HUVECs caused by high glucose.

aFGF inhibits high-glucose-induced EndMT by negatively regulating miR-155-5p

It is well known that various microRNAs play crucial roles in diabetic wounds. The literature review showed that miR-155 was significantly increased in a high-glucose environment and was regulated by FGF, which is involved in wound oxidative stress. Therefore, we focused on whether this factor participated in EndMT. To investigate the role of miR-155-5p in the inhibitory effects of aFGF on EndMT, we first examined the expression of miR-155-5p in a high-glucose environment and confirmed that miR-155-5p was highly expressed in HUVECs and that aFGF could partially reduce the expression of miR-155-5p (Figure 3A). We transfected miR-155-5p mimics and inhibitors and found that the proliferation (Figure 3B and M), migration (Figure 3F, I, K) and tube formation ability (Figure 3J, L) of HUVECs were increased by miR-155-5p inhibition compared with the effect of the mimic. In addition, in a high-glucose environment, the miR-155-5p inhibitor increased the expression of the vascular EC-specific markers VE-cadherin and CD31, whereas the expression of the mesenchymal markers α-SMA and Vim was decreased (Figure 3C, G). The pathological changes induced by EndMT were alleviated to some extent. In contrast, the miR-155-5p mimic decreased the expression of VE-cadherin and CD31 and increased the expression of a-SMA and Vim. aFGF partially reversed the pathological changes induced by EndMT (Figure 3D, H). We also performed fluorescent double-staining of cell-specific markers and mesenchymal markers, which further confirmed that the mimic intensified EndMT in HUVECs, and the inhibitor could alleviate EndMT in cells (Figure 4A, C). Next, we further verified the effects of miR-155-5p on total ROS levels, mitochondrial function and mtROS levels in cells. JC-1 staining showed that, compared with that in the mimic group, the MMP was significantly increased and mitochondrial damage was alleviated in the inhibitor group (Figure 4B). ROS and mtROS were significantly increased in cells exposed to the mimic, while the production of mtROS and ROS in these cells was inhibited in the miR-155-5p inhibitor group (Figure 4D–G). In summary, these findings confirmed that aFGF protected mitochondrial function and reduced cellular oxidative stress by negatively regulating miR-155-5p, thereby inhibiting high glucose-induced epithelial–mesenchymal transdifferentiation in HUVECs.

Luciferase targets the miR-155 downstream target gene SIRT1

We further investigated the exact mechanism by which miR-155-5p affects EndMT. A luciferase reporter gene assay was performed to confirm the targeting relationship. The miR-155-5p mimic significantly reduced luciferase activity in HEK293 cells transfected with reporter plasmids containing the SIRT1 wild-type 3′-UTR sequence ($p < 0.001$) compared with that in cells transfected with the negative control of the miR-155-5p mimic. However, the negative control of the mutant SIRT1 3′-UTR did not appear to be inhibited, which indicated the absence of binding (Figure 5A, B). Subsequently, HUVECs were transfected with the miR-155-5p mimic or inhibitor and the corresponding negative controls with Lipo2000 and were analysed by western blotting (Figure 5C, D) and fluorescence staining (Figure 5G–J). This analysis was performed to determine the relationship between miR-155-5p, SIRT1 and Nrf2/HO-1, which is a classic pathway that regulates oxidative stress. The results suggested that the expression of SIRT1 was increased in HUVECs that were transfected with the miR-155-5p inhibitor, and the corresponding mimic exerted the opposite effect. The expression of Nrf2 and HO-1 in the miR-155-5p mimic group was also inhibited, which was contrary to the effect of the inhibitor or aFGF on HUVECs. Moreover, there was a significant difference compared with the negative control ($p < 0.05$). These data indicate that SIRT1 is the direct target of miR-155-5p in high-glucose environments. aFGF alleviated oxidative stress via SIRT1/Nrf2/HO-1, reduced ROS levels, alleviated EndMT in HUVECs in high-glucose environments and ultimately improved the function of HUVECs.

Discussion

Difficulty in healing diabetic wounds and a high recurrence rate are the main causes of disability and death in patients with diabetes, which is becoming a major health problem worldwide [19]. The main reason for the difficulty in healing chronic diabetic wounds is the disturbance of the wound microenvironment caused by high glucose levels, which can lead to oxidative stress, vascular remodelling difficulties, peripheral neuropathy and chronic inflammation [20,21]. Vascular function provides nutrient and oxygen support throughout the wound healing process and plays an important role in chronic wound healing in diabetic patients [22]. However, high-glucose environments can induce high levels of ROS production, leading to functional defects in HUVECs, mitochondrial dysfunction in ECs, apoptosis and inflammation [23]. These changes ultimately manifest as impaired vascular function, reduced blood vessel density, insufficient production, limited extracellular matrix remodelling and delayed diabetic wound healing [3,24]. Although researchers have made great efforts to understand the causes of impaired healing in chronic diabetic wounds, the underlying molecular mechanism has not yet been fully

Downloaded from academic.oup.com/burnstrauma/article/doi/10.1093/burnst/tkae010/7683168 by guest on 13 October 2026

understood. At present, the treatment of diabetic wounds is not fully effective, and there is an urgent need for new therapeutic approaches to prevent and treat chronic diabetic wounds.

Previous studies have reported that aFGF, which was the first member of the FGF family discovered and is therefore also known as FGF-1, exerts a wide range of effects, including promoting mitosis in mesoderm- and ectoderm-derived cells; promoting the proliferation and migration of keratecyate cell (KCs), fibroblasts (FBs) and HUVECs; regulating the metabolism of collagen and the extracellular matrix; and promoting tissue repair and regeneration [3,25]. aFGF levels in natural tissues are very low [26]. In 2006, Li and colleagues developed recombinant human aFGF, which was the first aFGF drug in the world [27]. Subsequently, in clinical practice, recombinant human aFGF has been used in various studies of acute and chronic wounds. In recent years, several new mechanisms of action and indications for aFGF have been studied [28]. In this work, we investigated its role in the healing of diabetic wounds using a model of full-layer skin injury on the backs of db/db mice. aFGF inhibited oxidative stress in the skin, promoted angiogenesis and significantly accelerated wound healing in diabetic mice. New studies will undoubtedly provide additional insights into the key role of aFGF in chronic diabetic wounds.

The presence of a healthy endothelium plays a crucial role in the dynamic maintenance of vascular tension, angiogenesis and haemostasis and in providing anti-inflammatory, antioxidant and antithrombotic interfaces [29]. Endothelial dysfunction is a marker of many human vascular diseases, including atherosclerosis, vascular calcification, hypertension and diabetes [30]. A high-glucose environment in patients with diabetes leads to HUVEC dysfunction, resulting in reduced angiogenesis, which manifests as decreases in the density of blood vessels and capillaries [31]. In previous studies, we observed that HUVEC proliferation and migration were inhibited and angiogenesis was impaired under high-glucose conditions *in vitro* [32]. In this study, we evaluated the effects of aFGF on the proliferation, migration and tube formation of HUVECs under high-glucose conditions. aFGF significantly enhanced the proliferation and migration of HUVECs in high-glucose environments. Compared with those in the high-glucose group, more tube formation and more complete tubular structures were observed in aFGF-treated HUVECs. These results suggest that aFGF can enhance angiogenesis in high-glucose environments. Recent studies on the pathogenesis of VE cell dysfunction in patients with diabetes have shown that endothelial interstitial transformation is a novel feature of endothelial dysfunction [33]. This feature is characterized by the loss of cell-to-cell connections, a fibroblast-like morphology and fibrosis [34]. We performed fluorescence staining and analysed the protein expression of the vascular EC-specific markers VE-cadherin and CD31, as well as the mesenchymal markers α-SMA and Vim. The results confirmed that in high-glucose environments, the expression of VE-cadherin and CD31 decreased, whereas the expression of the mesenchymal markers α-SMA and Vim increased. aFGF partially reversed these pathological changes and ameliorated EndMT. Furthermore, EndMT can be induced by high oxidative stress in diabetic wounds, in which both the physical barrier and secretion functions of ECs are impaired. Mitochondria are the main sites of ROS production, and structural damage or dysfunction of these organelles can easily disrupt the *in vivo* balance and induce oxidative damage [35]. Harmful stimuli alter the permeability of the mitochondrial membrane, reduce membrane potential, block the transmission of the mitochondrial electron transport chain, inhibit the production of cytochrome c, inhibit the levels of adenosine triphosphate and accelerate the accumulation of total ROS in cells [36]. Based on the finding that aFGF could ameliorate oxidative stress in the wounds of animal models, this study confirmed that high glucose could induce abnormal changes in the MMP and the accumulation of mtROS and ROS in an *in vitro* high-glucose-induced VE cell model. Moreover, aFGF could improve the MMP of HUVECs in high-glucose environments, protect mitochondrial functions, clear mtROS and total ROS in cells, and alleviate oxidative stress in high-glucose environments, thereby improving EndMT.

miRNAs are a class of single-stranded noncoding RNAs containing 17–25 nucleotides that can influence gene expression at the posttranscriptional level [37]. There is growing evidence that miRNAs play a role in the pathogenesis and progression of diabetic wounds. The noncoding small RNA miR-155 is significantly increased in high-glucose environments and is affected by FGF regulation, thus participating in the oxidative stress response in wounds. Other researchers have indicated that miR-155 is closely related to EC dysfunction [38–40]. Our study revealed that miR-155-5p was highly expressed in high-glucose environments, and aFGF effectively reduced its expression. When cells were transfected with the miR-155-5p mimic, proliferation, migration and tube formation were also inhibited. EndMT-related protein assays and fluorescence staining confirmed that miR-155-5p promoted EC EndMT. In contrast, the miR-155-5p inhibitor increased the MMP, protected mitochondrial function, cleared mtROS and total ROS in cells, and reversed the pathological changes induced by EndMT. These findings further showed that aFGF inhibited the epithelial–mesenchymal transdifferentiation of HUVECs induced by high glucose by negatively regulating miR-155-5p, thus enhancing angiogenesis in high-glucose environments. The main function of miRNAs, which are a class of small endogenous noncoding RNAs, is to downregulate the expression of target genes by binding to the 3′-UTR [41,42]. Bioinformatic analysis revealed that miR-155-5p contained complementary sequences to the SIRT1 3′-UTR, and a luciferase reporter gene assay verified the targeted regulatory relationship between miR-155-5p and SIRT1. As expected, the miR-155-5p mimic significantly reduced luciferase activity in HEK293 cells transfected

Downloaded from academic.oup.com/burnstrauma/article/doi/10.1093/burnst/tkae010/7683168 by guest on 13 October 2026

with reporter plasmids containing SIRT1 wild-type 3′-UTR sequences.

It has been reported that Nrf2, which is an important transcription factor, inhibits oxidative stress by activating multiple genes encoding cytoprotective and antioxidant enzymes [43]. HO-1 is a key rate-limiting enzyme that catalyses the production of carbon monoxide, ferrous iron and biliverdin from haemoglobin. This protein is closely associated with oxidative stress and can be rapidly induced by various stressors, including oxidative stress, ultraviolet radiation and inflammatory cytokines. The regulation of the Nrf2/HO-1 defence axis is a classic pathway for alleviating oxidative stress in the body. Multiple studies have shown a direct connection between SIRT1 and the Nrf2/HO-1 signalling cascades, and SIRT1 can regulate the transcriptional activity of Nrf2 and its downstream targets [44,45]. In this study, we performed protein and fluorescence staining of factors in the SIRT1/Nrf2/HO-1 pathway, and the results showed that the miR-155-5p inhibitor promoted the expression of SIRT1, whereas the mimic exerted the opposite effect. The expression of Nrf2 and HO-1 in the miR-155-5p mimic group was also inhibited, further confirming that SIRT1 was a direct target of miR-155-5p in high-glucose environments. aFGF ameliorated oxidative stress via SIRT1/Nrf2/HO-1, which reduced the mtROS and ROS levels. The epithelial–mesenchymal transdifferentiation of HUVECs in high-glucose environments was thus alleviated, ultimately improving the function of HUVECs. This study focused on the effect of aFGF on vascular ECs in diabetic wounds and related mechanisms. *In vivo*, it is difficult to isolate wound vascular ECs, and it is difficult to determine whether the differential expression of certain factors is due to differences in vascular ECs in wounds. Therefore, *in vitro* studies on the mechanism of the aFGF/Nrf2/HO-1 pathway have been performed, but further animal experiments are lacking.

Conclusions

In conclusion, the results of our study indicated that aFGF enhanced the SIRT1/Nrf2/HO-1 pathway by inhibiting miR-155-5p. Furthermore, aFGF protected mitochondrial function and cleared mtROS, thereby reducing intracellular ROS levels and alleviating the pathological state of EndMT in HUVECs under high-glucose conditions. These results may be helpful for obtaining a comprehensive understanding of the relationship between aFGF and VE cell dysfunction in diabetic wounds, thereby providing support for the treatment of chronic diabetic wounds.

Abbreviations

aFGF: Acidic fibroblast growth factor; ECs: Endothelial cells; EndMT: Endothelial to mesenchymal transition; FGF: fibroblast growth factor; H&E: Hematoxylin and eosin; HUVECs: Human umbilical vein endothelial cells; miRNAs: MicroRNAs; MMP: Mitochondrial membrane potential; mtROS: Mitochondrial reactive oxygen species; PBS: Phosphate-buffered saline; ROS: Reactive oxygen species; SDS-PAGE: Sodium dodecyl sulphate-polyacrylamide gel electrophoresis; SMA: Smooth muscle actin; 3′UTR: 3′-Untranslated region; VE: Vascular endothelial.

Funding

This work was supported by the National Natural Science Foundation of China (81971835), the Shanghai Wang Zhengguo Foundation for Traumatic Medicine Growth Factor Rejuvenation Plan (SZYZ-TR-07) and the Key Industry Innovation Chain (Cluster)—Social Development Foundation of Shaanxi Province, China (2023-ZDLSF-37).

Authors' contributions

HW and DH designed the experiments and research methods; YZ, FH and YX performed the experiments and analysed study data; YL provided study materials, reagents and materials; JH replicated the results; and DH provided laboratory samples and animals. All authors read and approved the final manuscript.

Ethics approval and consent to participate

All animal procedures were carried out in accordance with the principles of ARRIVE and approved by the Ethics Committee of Fourth Military Medical University.

Conflict of interest

None declared.

Data availability

The data used to support the findings of this study are available from the corresponding author upon request.

References

1. Shaw JE, Sicree RA, Zimmet PZ. Global estimates of the prevalence of diabetes for 2010 and 2030. *Diabetes Res Clin Pract*. 2010;87:4–14.
2. Hart T, Milner R, Cifu A. Management of a Diabetic Foot. *JAMA*. 2017;318:1387–8.
3. Kathawala MH, Ng WL, Liu D, Naing MW, Yeong WY, Spiller KL, *et al*. Healing of Chronic Wounds: An Update of Recent Developments and Future Possibilities. *Tissue Eng Part B Rev*. 2019;25:429–44.
4. den Dekker A, Davis FM, Kunkel SL, Gallagher KA. Targeting epigenetic mechanisms in diabetic wound healing. *Transl Res*. 2019;204:39–50.
5. Zhang J, Chen S, Xiang H, Xiao J, Zhao S, Shu Z, *et al*. S1PR2/Wnt3a/RhoA/ROCK1/beta-catenin signaling pathway

Downloaded from academic.oup.com/burnstrauma/article/doi/10.1093/burnst/tkae010/7683168 by guest on 13 October 2026

promotes diabetic nephropathy by inducting endothelial mesenchymal transition and impairing endothelial barrier function. *Life Sci*. 2023;328:121853.
6. Yang S, Wang S, Chen L, Wang Z, Chen J, Ni Q, *et al*. Neutrophil Extracellular Traps Delay Diabetic Wound Healing by Inducing Endothelial-to-Mesenchymal Transition via the Hippo pathway. *Int J Biol Sci*. 2023;19:347–61.
7. Yan C, Grimm WA, Garner WL, Qin L, Travis T, Tan N, *et al*. Epithelial to mesenchymal transition in human skin wound healing is induced by tumor necrosis factor-alpha through bone morphogenic protein-2. *Am J Pathol*. 2010;176:2247–58.
8. Barriere G, Fici P, Gallerani G, Fabbri F, Rigaud M. Epithelial Mesenchymal Transition: a double-edged sword. *Clin Transl Med*. 2015;4:14.
9. Marconi GD, Fonticoli L, Rajan TS, Pierdomenico SD, Trubiani O, Pizzicannella J. Epithelial-Mesenchymal Transition (EMT): The Type-2 EMT in Wound Healing, Tissue Regeneration and Organ Fibrosis. *Cell*. 2021;10:1587.
10. Cronauer MV, Schulz WA, Seifert HH, Ackermann R, Burchardt M. Fibroblast growth factors and their receptors in urological cancers: basic research and clinical implications. *Eur Urol*. 2003;43:309–19.
11. Chen M, Bao L, Zhao M, Cao J, Zheng H. Progress in Research on the Role of FGF in the Formation and Treatment of Corneal Neovascularization. *Front Pharmacol*. 2020;11:111.
12. Wang HT, Han JT, Hu DH. Research advances on the role of acid fibroblast growth factor in promotion of wound healing. *Zhonghua Shao Shang Za Zhi*. 2022;38:859–63.
13. Sun J, Huang X, Niu C, Wang X, Li W, Liu M, *et al*. aFGF alleviates diabetic endothelial dysfunction by decreasing oxidative stress via Wnt/beta-catenin-mediated upregulation of HXK2. *Redox Biol*. 2021;39:101811.
14. Xiao L, Dudley AC. Fine-tuning vascular fate during endothelial-mesenchymal transition. *J Pathol*. 2017;241:25–35.
15. Roy O, Leclerc VB, Bourget JM, Thériault M, Proulx S. Understanding the process of corneal endothelial morphological change in vitro. *Invest Ophthalmol Vis Sci*. 2015;56:1228–37.
16. Li H, Jing S, Xu H. Effect and mechanism of microRNAs on various diabetic wound local cells. *J Diabetes*. 2023;15:955–67.
17. Feng J, Yao Y, Wang Q, Han X, Deng X, Cao Y, *et al*. Exosomes: Potential key players towards novel therapeutic options in diabetic wounds. *Biomed Pharmacother*. 2023;166:115297.
18. Xu WD, Feng SY, Huang AF. Role of miR-155 in inflammatory autoimmune diseases: a comprehensive review. *Inflamm Res*. 2022;71:1501–17.
19. Okonkwo UA, DiPietro LA. Diabetes and Wound Angiogenesis. *Int J Mol Sci*. 2017;18:1419.
20. Brownlee M. Biochemistry and molecular cell biology of diabetic complications. *Nature*. 2001;414:813–20.
21. Deng H, Li B, Shen Q, Zhang C, Kuang L, Chen R, *et al*. Mechanisms of diabetic foot ulceration: A review. *J Diabetes*. 2023;15:299–312.
22. Forrester SJ, Kikuchi DS, Hernandes MS, Xu Q, Griendling KK. Reactive Oxygen Species in Metabolic and Inflammatory Signaling. *Circ Res*. 2018;122:877–902.
23. Deng L, Du C, Song P, Chen T, Rui S, Armstrong DG, *et al*. The Role of Oxidative Stress and Antioxidants in Diabetic Wound Healing. *Oxidative Med Cell Longev*. 2021;2021:8852759.
24. Giacco F, Brownlee M. Oxidative stress and diabetic complications. *Circ Res*. 2010;107:1058–70.
25. Sluzalska KD, Slawski J, Sochacka M, Lampart A, Otlewski J, Zakrzewska M. Intracellular partners of fibroblast growth factors 1 and 2 - implications for functions. *Cytokine Growth Factor Rev*. 2021;57:93–111.
26. Phan P, Saikia BB, Sonnaila S, Agrawal S, Alraawi Z, Kumar TKS, *et al*. The Saga of Endocrine FGFs. *Cell*. 2021;10:2418.
27. Li XK. Seizing the day and living it to the full: thirty years' independent innovation of growth factors and wound repair. *Zhonghua Shao Shang Za Zhi*. 2020;36:161–5.
28. Yamakawa S, Hayashida K. Advances in surgical applications of growth factors for wound healing. *Burns Trauma*. 2019;7:10.
29. Xiang L, Mittwede PN, Clemmer JS. Glucose Homeostasis and Cardiovascular Alterations in Diabetes. *Compr Physiol*. 2015;5:1815–39.
30. Brownlee M. The pathobiology of diabetic complications: a unifying mechanism. *Diabetes*. 2005;54:1615–25.
31. Li JM, Shah AM. Endothelial cell superoxide generation: regulation and relevance for cardiovascular pathophysiology. *Am J Physiol Regul Integr Comp Physiol*. 2004;287:R1014–30.
32. Zhang Y, Bai X, Shen K, Luo L, Zhao M, Xu C, *et al*. Exosomes Derived from Adipose Mesenchymal Stem Cells Promote Diabetic Chronic Wound Healing through SIRT3/SOD2. *Cell*. 2022;11:2568.
33. Lu D, Jiang H, Zou T, Jia Y, Zhao Y, Wang Z. Endothelial-to-mesenchymal transition: New insights into vascular calcification. *Biochem Pharmacol*. 2023;213:115579.
34. Immanuel J, Yun S. Vascular Inflammatory Diseases and Endothelial Phenotypes. *Cell*. 2023;12(12):1640.
35. Kluge MA, Fetterman JL, Vita JA. Mitochondria and endothelial function. *Circ Res*. 2013;112:1171–88.
36. Jarmuszkiewicz W, Dominiak K, Budzinska A, Wojcicki K, Galganski L. Mitochondrial Coenzyme Q Redox Homeostasis and Reactive Oxygen Species Production. *Front Biosci (Landmark Ed)*. 2023;28:61.
37. Dinesen S, El-Faitarouni A, Frisk NLS, Sørensen AE, Dalgaard LT. Circulating microRNA as Biomarkers for Gestational Diabetes Mellitus-A Systematic Review and Meta-Analysis. *Int J Mol Sci*. 2023;24(7):6186.
38. Gao J, Zhao G, Li W, Zhang J, Che Y, Song M, *et al*. MiR-155 targets PTCH1 to mediate endothelial progenitor cell dysfunction caused by high glucose. *Exp Cell Res*. 2018;366:55–62.
39. Moura J, Sørensen A, Leal EC, Svendsen R, Carvalho L, Willemoes RJ, *et al*. microRNA-155 inhibition restores Fibroblast Growth Factor 7 expression in diabetic skin and decreases wound inflammation. *Sci Rep*. 2019;9:5836.
40. Sonkoly E, Janson P, Majuri ML, Savinko T, Fyhrquist N, Eidsmo L, *et al*. MiR-155 is overexpressed in patients with atopic dermatitis and modulates T-cell proliferative responses by targeting cytotoxic T lymphocyte-associated antigen 4. *J Allergy Clin Immunol*. 2010;126:581–589.e20.
41. Li Y, Zhang J, Shi J, Liu K, Wang X, Jia Y, *et al*. Exosomes derived from human adipose mesenchymal stem cells attenuate hypertrophic scar fibrosis by miR-192-5p/IL-17RA/Smad axis. *Stem Cell Res Ther*. 2021;12:221.
42. Baek D, Villén J, Shin C, Camargo FD, Gygi SP, Bartel DP. The impact of microRNAs on protein output. *Nature*. 2008;455:64–71.

Downloaded from academic.oup.com/burnstrauma/article/doi/10.1093/burnst/tkae010/7683168 by guest on 13 October 2026

43. Mohan S, Gupta D. Crosstalk of toll-like receptors signaling and Nrf2 pathway for regulation of inflammation. *Biomed Pharmacother*. 2018;108:1866–78.
44. Shen K, Jia Y, Wang X, Zhang J, Liu K, Wang J, *et al*. Exosomes from adipose-derived stem cells alleviate the inflammation and oxidative stress via regulating Nrf2/HO-1 axis in macrophages. *Free Radic Biol Med*. 2021;165:54–66.
45. Sethi P, Mehan S, Khan Z, Chhabra S. Acetyl-11-keto-beta boswellic acid(AKBA) modulates CSTC-pathway by activating SIRT-1/Nrf2-HO-1 signalling in experimental rat model of obsessive-compulsive disorder: Evidenced by CSF, blood plasma and histopathological alterations. *Neurotoxicology*. 2023;98: 61–85.

Downloaded from academic.oup.com/burnstrauma/article/doi/10.1093/burnst/tkae010/7683168 by guest on 13 October 2026